



# Bentonite-Polysorbate 80 for Removal CI Direct Blue 1 and CI Direct Yellow 4

Jindrayani Nyoo Putro<sup>1,2</sup> · Felycia Edi Soetaredjo<sup>1,2</sup> · Christian Julius Wijaya<sup>1,2</sup> · Shella Permatasasri Santoso<sup>1,2</sup> · Chintya Gunarto<sup>1,2</sup> · Agus Saptoro<sup>3</sup> · Jaka Sunarso<sup>4</sup> · Sanggono Adisasmito<sup>5</sup> · I. Gede Wenten<sup>5</sup> · Suryadi Ismadji<sup>1,2</sup>

Received: 15 April 2024 / Accepted: 10 September 2024 / Published online: 21 September 2024  
© The Tunisian Chemical Society and Springer Nature Switzerland AG 2024

## Abstract

The non-ionic surfactant Polysorbate-80, often known as Tween-80, was employed to increase the adsorption capacity of natural bentonite. The procedure of modifying bentonite was conducted using microwave radiation. The intercalation of polysorbate-80 increased the basal spacing of bentonite from 1.54 to 1.66 nm. The bentonite's BET surface area is 72.6 m<sup>2</sup>/g, accompanied by a total pore volume of 0.61 cm<sup>3</sup>/g. In contrast, the BET surface area of bentonite-polysorbate 80 is determined to be 84.2 m<sup>2</sup>/g, with a total pore volume of 0.72 cm<sup>3</sup>/g. The adsorption kinetics of direct blue-1 (DB-1) and direct yellow-4 (DY-4) on bentonite and bentonite-polysorbate 80 may be accurately described by the pseudo-second-order model. Furthermore, the adsorption isotherms data for both dyes can be best fitted using the Langmuir equation. A proposed modification of the extended Langmuir model was suggested as a means to enhance the efficacy of this model in correlating binary adsorption data. Incorporating the competition parameter into the affinity coefficient parameter of the Langmuir equation allows for the representation of the binary adsorption of DB-1 and DY-4.

**Keywords** Binary adsorption · Competition parameter · Affinity coefficient · Intercalation · Interlayer spacing

## 1 Introduction

The ecological integrity of Earth's ecosystems is contingent upon the presence of water, an essential and irreplaceable constituent of the cosmos. Water scarcity is a persistent concern in both industrialized and developing countries. The

issue of water shortage and clean water is anticipated to affect an increasing number of people worldwide soon due to water pollution. Water contamination caused by industrial activity is a pressing global issue that needs urgent action. Water pollution often poses significant challenges for human populations and the natural environment. These challenges encompass a range of issues, including the contamination of drinking water sources, the pollution of animal feed, and the disruption of fragile ecosystems in lakes and rivers, which can have detrimental effects on biodiversity, among other consequences. Synthetic dyes are the main contributor to pollution in aquatic ecosystems. Several dyes resist degradation, threatening both human health and aquatic ecosystems. According to Ismadji et al. [13], the presence of pigments in water can be detected even at low concentrations, and their ability to obstruct the transmission of light has the potential to diminish the diversity of aquatic organisms.

Different varieties of dyes are currently available on the market. They can be categorized according to the following criteria: natural dyes, synthetic dyes, direct dyes, dispersed dyes, reactive dyes, and solvent dyes. Direct dyes exhibit superior colorfastness compared to other dyes; therefore, this type of dye is widely used for coloring linen, wool, cotton,

✉ Suryadi Ismadji  
suryadiismadji@yahoo.com

<sup>1</sup> Department of Chemical Engineering, Widya Mandala Surabaya Catholic University, Kalijudan 37, Surabaya 60114, Indonesia

<sup>2</sup> Collaborative Research Center for Zero Waste and Sustainability, Jl. Kalijudan 37, Surabaya, East Java 60114, Indonesia

<sup>3</sup> Department of Chemical and Energy Engineering, Curtin University Malaysia, CDT 250, 98009 Miri, Sarawak, Malaysia

<sup>4</sup> Research Centre for Sustainable Technologies, Faculty of Engineering, Computing and Science, Swinburne University of Technology, 93350 Kuching, Malaysia

<sup>5</sup> Department of Chemical Engineering, Institut Teknologi Bandung, Jl. Ganesha 10, Bandung 40132, Indonesia

silk, rayon, and nylon [13]. Direct dyes represent a category of synthetic dyes that significantly contribute to the issue of water pollution stemming from dyeing processes. Direct dyes can be immediately applied to the material intended for coloring in neutral or alkaline solutions. Cellulose and cotton fibers are commonly dyed with direct dyes, which are affordable synthetic colors. Applying this dye to linen and cotton produces a vibrant coloration without needing a mordant. Additionally, it possesses the capability to dye rayon fibers effectively. Direct dyes exhibit an instantaneous and intense chromatic effect. However, their colorfastness significantly declines, particularly following multiple laundering cycles. Over time, these hues permeate the network of rivers and contribute to environmental contamination, particularly when the water is not subjected to prior treatment [13, 22].

An adsorption process is a highly effective method for treating effluent-containing dyes. The success of the adsorption process in removing dyes from wastewater depends on the adsorbent used. Various nanomaterial-based adsorbents have been developed and investigated for their efficacy in removing dyes from wastewater. These nanomaterial-based adsorbents include metal–organic frameworks and their modified forms [9, 11, 16, 31], magnetic-based materials [10, 12, 21], clay materials based [1, 19], carbon-based materials [4, 25], and agricultural waste materials [20]. Some of these materials have a high adsorption capacity and efficacy. Still, their raw materials and manufacturing processes are expensive and unsuitable for industrial applications.

Wastewater that contains dyes and enters the wastewater treatment system typically exhibits a mixture of multiple dyes rather than just one. Hence, it is imperative to investigate the adsorption of dyes from artificial wastewater, which contains more than a single dye. Multiple investigations have been conducted on binary dye systems using different adsorbents to study the dye adsorption process. Yazid et al. [28] recently studied binary adsorption of malachite green and safranin using activated carbon from walnut shells. The authors used density functional theory to correlate their experimental data. Based on the theoretical study, malachite green is more electrophilic than safranin. As a result, it exhibits stronger interaction with surface sites in both simple and binary systems, leading to removal rates of 93.12% and 78.41%, respectively. Both systems attained optimal removal outcomes at a pH level of 7. Other recent studies on the adsorption of dyes binary mixtures are as follows: indigo carmine and congo red onto Nickel–Chromium and Zinc–Chromium layered double hydroxides [2], indigo blue and sulfur black onto Zinc@magnetite [27], methylene blue and methyl orange onto chitosan nanoparticles [5], etc.

Clay minerals are among the most prevalent substances on this planet. These minerals are crucial to the advancement of human civilization. Clay minerals are used extensively to

manufacture various household appliances, raw materials for buildings, ceramics, industrial raw materials, and others. Clay minerals are utilized to dispose of and store toxic substances for environmental protection. Cation exchange capacity (CEC) measures clay minerals' ability to retain harmful chemicals. The hazardous compounds are bound to the clay minerals by either adsorption or ion exchange mechanisms. One of the essential groups in clay minerals for adsorption process applications is smectite. Substitution in the octahedral and a few tetrahedral sheets is a distinguishing feature of smectite clay with other clay minerals. Magnesium and iron replace aluminum in octahedral sheets, while aluminum replaces silicon in tetrahedral sheets. Montmorillonite or bentonite is a critical clay in the smectite group and has been used as an adsorbent in many laboratory or industrial applications. Bentonite's silicate-alumina triple-layer structure has a permanent negative surface charge, typically balanced by exchangeable  $\text{Na}^+$  and  $\text{Ca}^{2+}$  cations. This negative surface charge attracts oppositely charged molecules [13].

The CEC value of bentonite is very dependent on the mine location. Bentonite with a high CEC value can be used directly as an adsorbent. Still, bentonite with a low CEC value requires a modification process before it can be used as an effective adsorbent. Modification of bentonite as an adsorbent for dyes can be done by various methods, such as activation with acid [18], modification with natural polymers [1], combination with enzyme and other nanomaterials [17], combination with other materials to form composites [26], intercalation with surfactants [24, 30, 32], etc.

In this study, to improve the adsorption ability of bentonite (Ca-bentonite) on CI Direct Blue 1 (DB-1) and CI Direct Yellow 4 (DY-4) dyes, a modification was made using non-ionic surfactant polysorbate 80 or Tween 80. DB-1 and DY-4 are widely used direct dyes in industries. The choice of polysorbate-80 as a surfactant is based on the availability of this substance for industrial use so that the resulting composite can also be used on an industrial scale. So far, there is no study on the absorption ability of bentonite-polysorbate 80 composites against DB-1 and DY-4. Kinetics, equilibrium, and thermodynamics of DB-1 and DY-4 adsorption on bentonite-polysorbate 80 are also discussed in detail in this paper. In addition, a modification was made to the extended Langmuir equation to represent the binary adsorption isotherm of DB-1 and DY-4 on bentonite and bentonite-polysorbate 80.

## 2 Materials and Methods

### 2.1 Materials

This study's raw material was calcium bentonite from a bentonite mine in Ponorogo, East Java, Indonesia. Non-ionic

surfactant polysorbate-80 ( $C_{64}H_{124}O_{26}$ ), CI Direct Blue 1 ( $C_{34}H_{24}N_6Na_4O_{16}S_4$ , an anionic dye), and CI Direct Yellow 4 ( $C_{26}H_{20}N_4O_8S$ , anionic disodium salt) were purchased from Sigma-Aldrich. Hydrogen peroxide solution (50%), NaCl, and hydrochloric acid (37%) were obtained from the chemical store in Surabaya.

## 2.2 Pretreatment of Bentonite

The moisture content of bentonite recovered straight from the mining site was roughly 56%. The bentonite used in this study is of middle quality and contains several contaminants, necessitating preliminary pretreatment before its application. Before being used as a raw material for creating composites, pretreatment should be done beforehand to increase processing efficiency. The initial stage of bentonite processing was drying to 15% moisture content (to limit the rise of acidity during storage), followed by size reduction (100/120 mesh). Drying was carried out using a forced circulation oven at 105 °C until the desired moisture content was reached, followed by size reduction using porcelain mortar. The next step was to remove organic impurities with a hydrogen peroxide solution. At this stage, 500 ml of hydrogen peroxide solution was added to 100 g of bentonite while slowly stirred for 2 h. Bentonite was rinsed with RO water repeatedly to remove excess  $H_2O_2$ . Then bentonite was put into 500 ml of 2 N hydrochloric acid solution while stirring at 100 rpm for 6 h. After the acid activation process, the bentonite was rinsed repeatedly to remove excess acid attached to the bentonite. Moreover, the bentonite employed for subsequent experiments is acid-activated.

The mono-ionic properties of bentonite were improved using the following procedure: 50 g of bentonite was mixed into 250 mL of 1 N NaCl solution while stirring at 200 rpm for 1 h. Subsequently, the bentonite was separated from the solution and reacted again with 250 mL of NaCl solution for 1 h, accompanied by stirring. This process was carried out successively five times. After the process, the bentonite was separated from the solution and washed with RO water until chloride ions were not detected by adding silver nitrate solution. Bentonite was dried at 105 °C to 12% moisture content and pulverized using a porcelain mortar and sieve to a size of 100/120 mesh.

## 2.3 Cation Exchange Capacity (CEC) Determination

The bentonite's cation exchange capacity (CEC) was measured using the ASTM C837-99 method. The results showed that the initial CEC of bentonite and bentonite that had gone through the pretreatment process were 37.5 meq/100 g and 57.3 meq/100 g, respectively. CEC bentonite-polysorbate 80 was measured according to the ASTM C837-99 method, and the result was 34.4 meq/100 g. The decrease in CEC

value after modification occurred because some cations were released or replaced from the bentonite interlayer during modification with polysorbate-80.

## 2.4 Bentonite-Polysorbate 80 Preparation

The procedure for making bentonite-polysorbate 80 can be briefly described as follows: 25 g of bentonite was added to 250 mL of surfactant solution (concentration of 2% by weight). Then, the suspension was stirred at 200 rpm for 3 h. Then, the suspension was transferred to a microwave oven (LG, Model MS2042DB). The microwave was run at a frequency of 2.45 GHz at a power of 900 W for 5 min. The solid was then separated from the solution by centrifugation. The solids were repeatedly washed with RO water until free of surfactants (constant pH of washing water), dried at 105 °C for 24 h, and crushed to a 100/120 mesh particle size. The concentration of polysorbate-80 remaining in the solution was determined by the HPLC method using the C18 column; by knowing the remaining, the percentage of polysorbate-80 bounded in the composite can be determined. The percentage of polysorbate-80 bounded in the composite was  $73 \pm 6.2\%$ . The mobile phase used in HPLC analysis was a mixture of acetonitrile, water, and trifluoro acetic acid with a volume ratio of 81:19:0.1. The flow rate of the mobile phase used was 0.6 mL/min with the column temperature maintained at 30 °C, and the injection volume was 20  $\mu$ L. The analysis duration was approximately 10 min. The detection was carried out at a wavelength of 200 nm.

## 2.5 Characterization of Bentonite and Bentonite-Polysorbate 80 Composite

Utilizing scanning electron microscopy (SEM), the surface topography of the bentonite and bentonite-polysorbate 80 composites were analyzed. The adsorbents' surface topography was observed using a JEOL JSM-6390 field emission SEM with an accelerating voltage of 20 kV. The KBr disk technique was used for FT-IR analysis on a Shimadzu FTIR 8400S spectrometer. In transmission mode, 200 transmission measurements with a spectral resolution of 4  $cm^{-1}$  were accumulated over a wavenumber range of 4000–400  $cm^{-1}$  to obtain spectrum data. Data were spectrally adjusted, normalized, and smoothed using IRsolution software.

The mineralogical composition of bentonite and bentonite-polysorbate 80 was analyzed using the X-ray diffraction method (Philips PANalytical X'Pert X-ray diffractometer). Powder diffractograms of bentonite and bentonite composites were obtained at 40 kV and 30 mA at an angle range of  $2\theta$  ( $5^\circ$ – $50^\circ$ ) with a scanning speed of 1  $min^{-1}$ . The radiation source was Ni-filtered  $CuK\alpha_1$  ( $\lambda = 0.15405$  nm).

The pore structure of bentonite and bentonite-polysorbate 80 was characterized using nitrogen gas adsorption

at the gas boiling point. Before the adsorption–desorption procedure, the adsorbents were degassed to remove trapped gases and free moisture content from the structure of the internal pores. The degassing process was conducted for 24 h at a vacuum pressure and temperature of 120 °C. The adsorption and desorption of nitrogen gas onto and from the two adsorbents were conducted at relative pressures ( $p/p_o$ ) ranging from  $10^{-5}$  to 0.999. The active surface area of the adsorbents was calculated using the BET method at a relative pressure range of 0.05 to 0.3. The pore volume was determined at the highest relative pressure in the experiment. Utilizing the ASAP-2000 Micromeritics Sorption Analyzer, a nitrogen sorption analysis was conducted.

## 2.6 Adsorption Studies

Both adsorption kinetics and isotherms of dyes were conducted in a batch system. The dye solutions were prepared by dissolving a certain amount of DB-1 and DY-4 in 1 L of deionized water to produce an initial concentration of 250 mg/L. In the adsorption isotherm experiment, 100 mL of DB-1 or DY-4 solutions were poured into several blue cap-stoppered bottle glasses containing an adsorbent with a known mass (0.1–1 g). Then, the stoppered bottle glasses were placed in a shaking water bath and shaken at 100 rpm for 24 h. The preliminary experiments showed that the equilibrium time for the two dyes used in the adsorption process using bentonite or bentonite-polysorbate 80 was less than 24 h. Adsorption isotherm experiments were conducted at 30, 40, and 50 °C. An integrated PID-type temperature controller kept the temperature in the water bath constant. The initial pH of the solution for the adsorption experiment was 6.8 (best adsorption condition).

After reaching equilibrium, the solid is separated from the suspension by centrifugation at 6000 rpm for 10 min. The supernatant obtained was then analyzed using a Shimadzu UV–Vis spectrophotometer to determine the remaining dye in the solution with a detection wavelength of 565 nm for DB-1 and 497 nm for DY-4. The amount of dye adsorbed ( $q_e$  (mg/g)) by bentonite or bentonite-polysorbate 80 at equilibrium was calculated using Eq. (1).

$$q_e = \frac{C_o - C_e}{m} V \quad (1)$$

Symbols  $C_o$  (mg/L) and  $C_e$  (mg/L) represent initial and equilibrium concentrations of dye, respectively. Symbols  $m$  (in g) and  $V$  (in L) represent the mass of the adsorbent and solution volume, respectively.

The adsorption kinetics experiment was conducted with the same procedure as the isotherm experiment. The

difference with adsorption isotherms is in collecting and analyzing samples at a specific time. The amount of dye adsorbed at a certain time ( $q_t$ ) was determined by Eq. (2).

$$q_t = \frac{C_o - C_t}{m} V \quad (2)$$

where  $C_t$  is dye concentration at time  $t$ .

## 2.7 Binary Adsorption Experiment

In industrial-scale wastewater treatment, dyestuff liquid waste is rarely found in single compound conditions, usually a mixture of several colors at once. Therefore, conducting adsorption studies involving more than one component is necessary. In this study, the adsorption of DB-1 and DY-4 was carried out not only as a single component but also as a binary one. The effect of competition between dyestuffs is also studied in this binary adsorption.

The binary adsorption experimental procedure is broadly the same as single component adsorption. The difference is that the two dyes, DB-1 and DY-4, were mixed with a specific initial concentration and put into a stoppered glass bottle containing a specific weight of adsorbent. The equilibrium concentrations of DB-1 and DY-4 were measured spectrophotometrically in the multi-component quantization method at two measurement wavelengths of 565 nm and 497 nm. The calibration curves were constructed using five standards containing pristine DB-1 and DY-4. The equilibrium concentration of DB-1 and DY-4 in a multi-component system was calculated based on Zeinali et al. [29].

## 3 Results and Discussion

### 3.1 Characterization of Adsorbents

The surface topography of bentonite and bentonite-polysorbate 80 composites obtained from characterization using SEM can be seen in Fig. 1. This figure shows that the surface topography of the initial bentonite and the bentonite after modification with the non-ionic surfactant polysorbate-80 did not significantly change. The addition of surfactants to bentonite will alter the structure of the adsorbent interlayer, but these alterations cannot be detected using SEM analysis.

FTIR spectra of bentonite, polysorbate 80, and bentonite-polysorbate 80 are depicted in Fig. 2. Several functional groups characteristic of montmorillonite are found in the FTIR spectrum of bentonite. Montmorillonite is the main constituent clay mineral present in bentonite. The wavenumber of  $3538 \text{ cm}^{-1}$  corresponds to the O–H stretch for  $\text{H}_2\text{O}$  in the silica matrix, while the O–H stretch of the silanol (Si–OH) group is represented by the

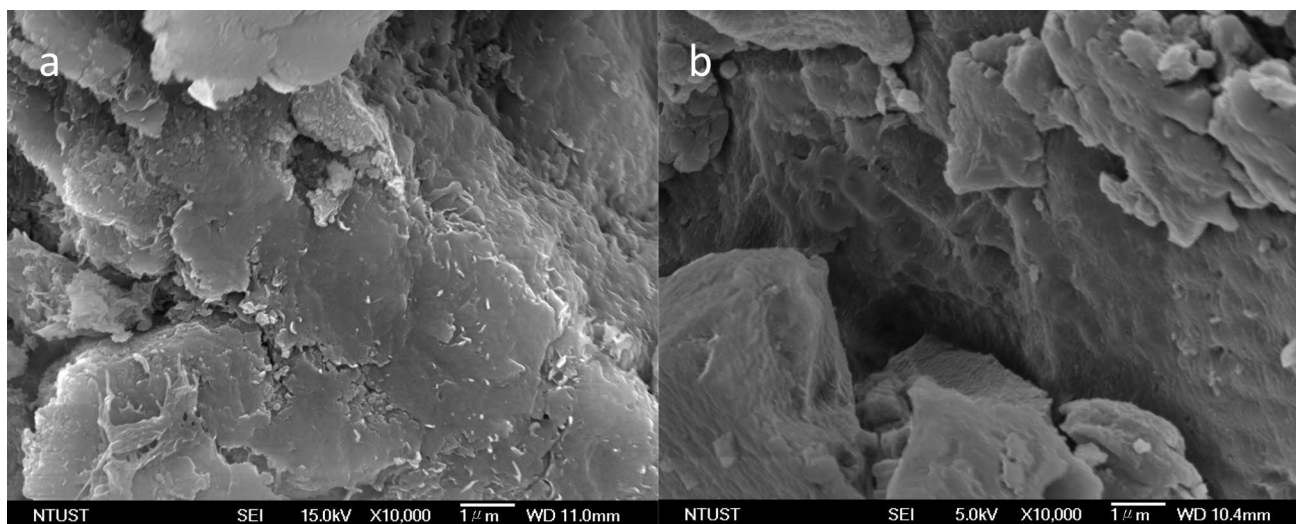


**Fig. 1** SEM images of: **a** bentonite, and **b** bentonite-polysorbate 80 composite

wavenumber of  $3275\text{ cm}^{-1}$ . The O–H functional group bend for adsorbed  $\text{H}_2\text{O}$  at bentonite interlayer is shown in wavenumber  $1666\text{ cm}^{-1}$ . A wavenumber of  $1036\text{ cm}^{-1}$  indicates the Si–O–Si stretch of the tetrahedral sheet. The other three functional groups, Al–Al–OH bend, Al–O–Si bend (for octahedral Al), and Si–O–Si bend, are indicated by wavenumbers of 921, 692, and  $438\text{ cm}^{-1}$ , respectively [14]. In the FTIR spectrum, the main characteristics of polysorbate 80 can be seen in wavenumbers  $3100\text{--}3700$ , 1736, and  $1112\text{ cm}^{-1}$ , which are related to the O–H stretching

vibration, asymmetric C=O, and C–O vibration stretching groups, respectively [6], furthermore, the band around  $2850$  to  $2866\text{ cm}^{-1}$  is  $-\text{CH}_2$  vibrations (for symmetric stretching vibrations). All montmorillonite characteristics were found in the FTIR spectrum of bentonite-polysorbate 80, and one of the functional groups belonging to polysorbate-80 (C=O stretching vibrations) appeared in the composite. This evidence indicates that polysorbate 80 was contained in a bentonite structure. Intercalation of the polysorbate functional group into the interlayer bentonite possibly occurred.

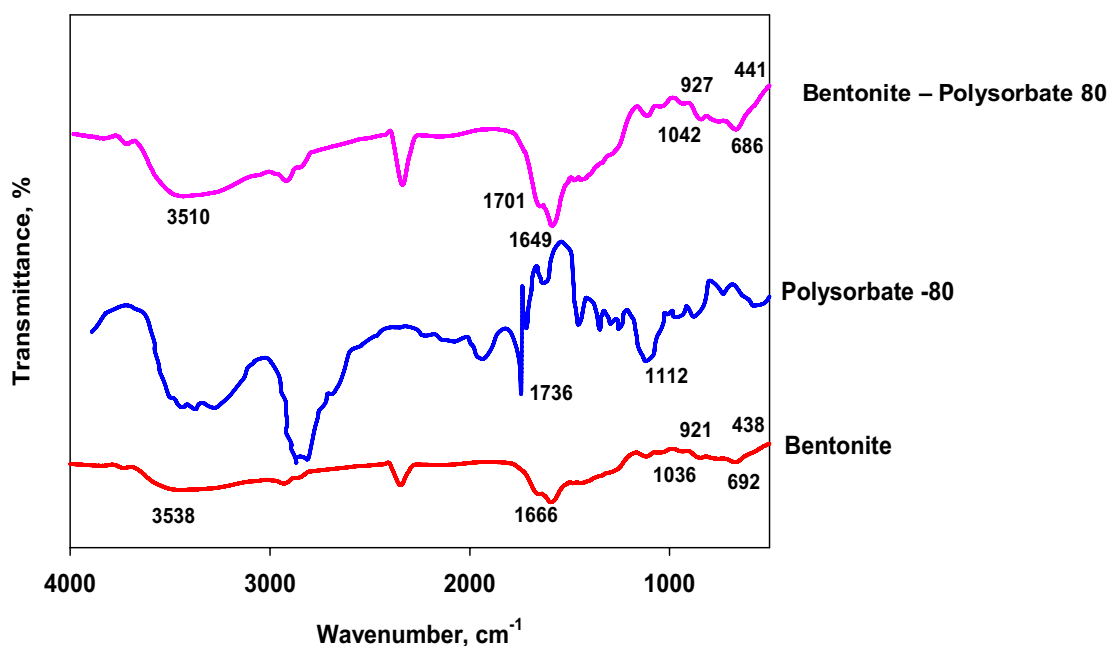


**Fig. 2** FTIR spectra of bentonite, polysorbate 80, and bentonite-polysorbate 80 composite

Figure 3 reveals that the XRD diffractogram of bentonite consists of several clay minerals. Bentonite is a clay made up of a varied combination of substances, including montmorillonite, illite, and additional elements such as cristobalite, quartz, carbonates, feldspars, and trace quantities of iron oxy-hydroxides [8]. The main characteristic of montmorillonite is a diffraction peak at (001) basal reflection. The diffraction peak, corresponding to (001) basal reflection for bentonite, was observed at  $2\theta$  around  $5.76^\circ$ , while the bentonite-polysorbate 80 was observed at  $2\theta$  around  $5.32^\circ$ . The basal spacing ( $d_{001}$ ) can be calculated using Bragg's equation as follows:

$$d = \frac{\lambda}{2\sin\theta} \quad (3)$$

where  $\lambda$  is the X-ray wavelength and  $\theta$  is the scattering angle for the peak position. The basal spacing for bentonite is 1.54 nm, and the bentonite-polysorbate 80 is 1.66 nm. The increase of basal spacing in composite due to the intercalation of polysorbate-80 into the interlayer of bentonite. The data presented in Fig. 3 demonstrates that purifying raw bentonite using hydrogen peroxide did not alter its basal spacing. Similarly, the basal spacing remains unchanged in bentonite that has undergone acid activation.

Nitrogen sorption isotherms for both bentonite and bentonite-polysorbate 80 are shown in Fig. 4. According to the IUPAC classification, nitrogen gas adsorption and desorption profiles on bentonite and composite are type IV with a H3 hysteresis loop. As depicted in Fig. 4 (inset), the pore size distribution range of materials of this type is relatively broad, with mesoporous pores predominating

over micropores. Adsorbent pore size distributions were determined using DFT (density functional theory). Figure 4 shows a capillary condensation phenomenon in some mesopores with large sizes and macropores, as indicated by a sudden increase in nitrogen adsorption at relative pressures ( $p/p_o$ ) greater than 0.90. The surface area of both adsorbents was determined using the BET method at  $p/p_o$  of 0.05 to 0.3. The BET surface area of bentonite is  $72.6 \text{ m}^2/\text{g}$ , with a total pore volume of  $0.61 \text{ cm}^3/\text{g}$ . Intercalation of polysorbate-80 into the interlayer of bentonite increased the BET surface area and total pore volume. The BET surface area of bentonite-polysorbate 80 is  $84.2 \text{ m}^2/\text{g}$ , and the total pore volume is  $0.72 \text{ cm}^3/\text{g}$ .

### 3.2 Adsorption Kinetics

Knowing how quickly a system can attain equilibrium is necessary to understand an adsorption process comprehensively. Experiments on adsorption kinetics can provide this information. The adsorption kinetics experiment yielded information regarding the amount of solute adsorbed per gram of adsorbent as a function of time. Then, these data were processed further with various adsorption kinetic equations to obtain information on time constants and equilibrium conditions.

The adsorption kinetics models utilized in this investigation are pseudo-first-order (PFO) and pseudo-second-order (PSO). Lagergren devised the PFO model over a century ago [15]. Consequently, this PFO model is commonly known as the Lagergren model. The pseudo-second-order model (PSO) was devised by Blanchard et al. [7] long after the

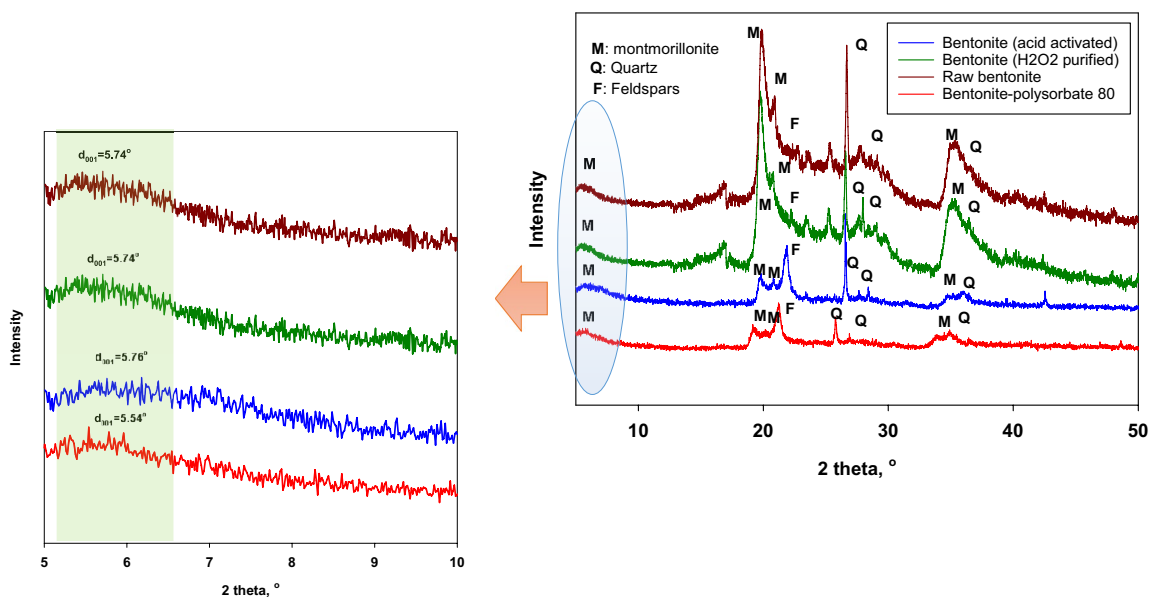


Fig. 3 XRD diffractograms of raw bentonite, purified  $\text{H}_2\text{O}_2$  bentonite, bentonite (acid activated), and bentonite-polysorbate 80

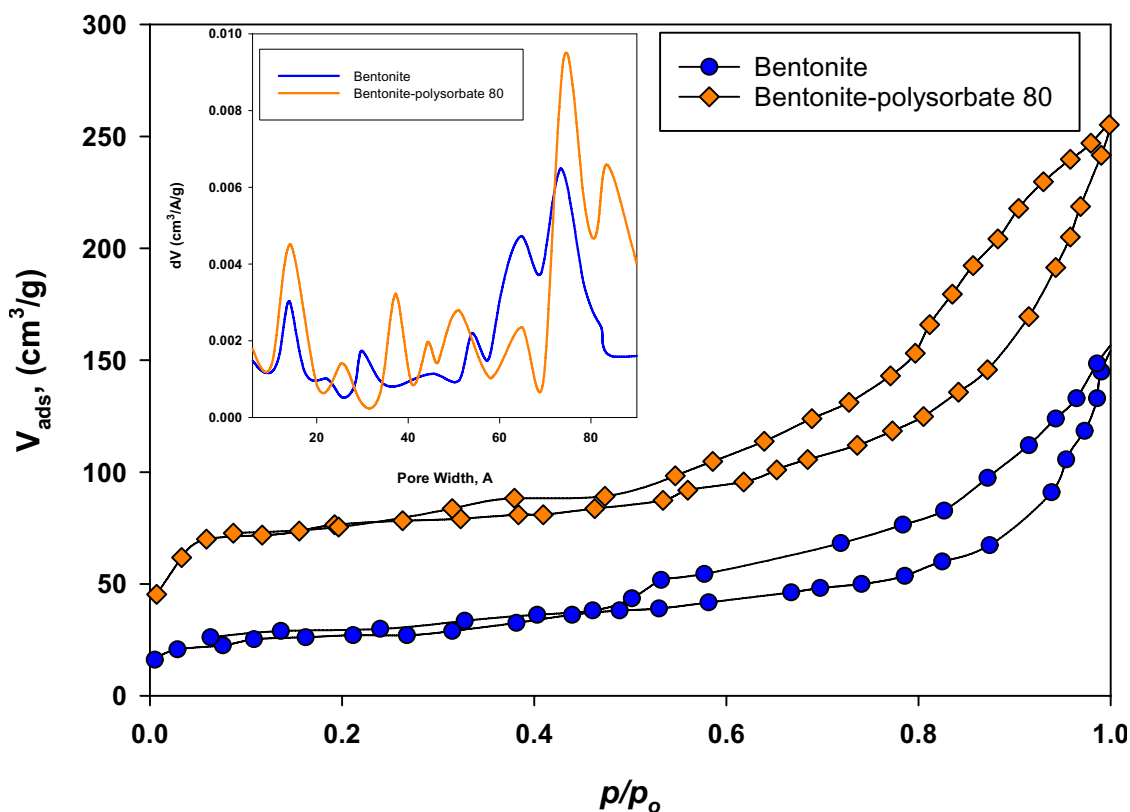


Fig. 4 Nitrogen sorption isotherms and pore size distribution of bentonite and bentonite-polysorbate 80

Lagergren model. The PFO mathematically can be expressed as:

$$q_t = q_e(1 - \exp(-k_1t)) \tag{4}$$

PSO kinetic has the form as follows:

$$q_t = \frac{q_e^2 k_2 t}{(1 + q_e k_2 t)} \tag{5}$$

where  $q_t$  is the amount of solute adsorbed at time  $t$ ,  $k_1$  is the time constant for the PFO, and  $k_2$  is the time constant for the PSO model.

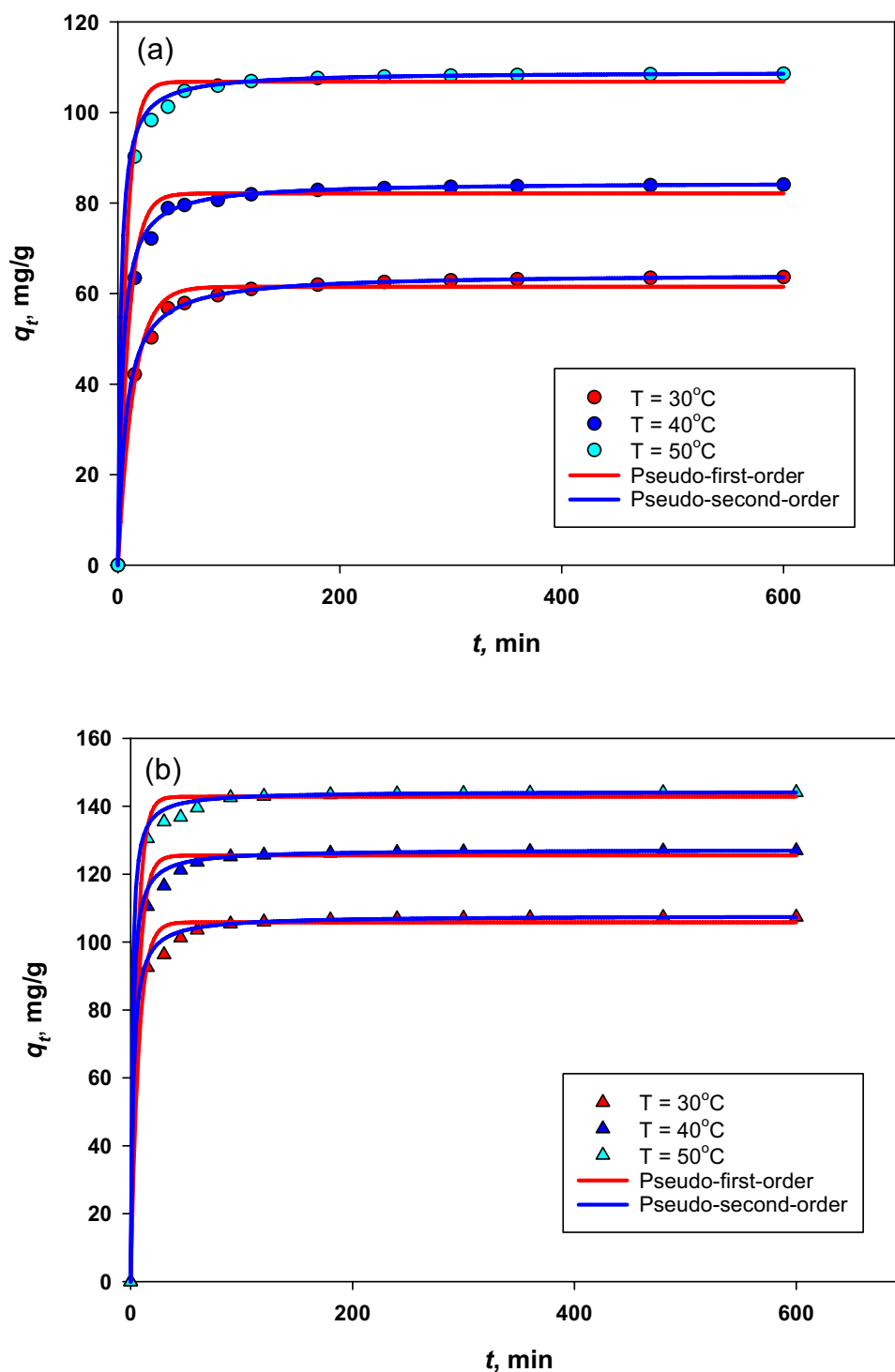
Figures 5 and 6 depict experimental data on the DB-1 and DY-4 adsorption kinetics on bentonite and bentonite-polysorbate 80, respectively. The same figures also display the results of calculations based on PFO and PSO equations that model adsorption kinetics. In the meantime, Table 1 shows the parameters of the PFO and PSO equations derived by fitting the experimental data. Those two equations represent DB-1 and DY-4 adsorption kinetics data on bentonite and bentonite-polysorbate 80.

Determining an equation that can represent experimental data on a system's adsorption kinetics should rely not solely on the regression coefficient  $R^2$  but also on the obtained

parameter values. The values of the parameters obtained must meet the requirements of the equation and have a physical meaning. Parameters  $k_1$  and  $k_2$  of the PFO and PSO equations indicate how quickly a system reaches equilibrium. The higher the value of these parameters, the quicker the system will achieve equilibrium. The values of these two parameters depend on the operating conditions, such as the solution's initial concentration, temperature, and pH. As summarized in Table 1, the effect of temperature on these two parameters is obvious. The values of  $k_1$  and  $k_2$  are consistent; both parameters,  $k_1$  and  $k_2$ , increase with increasing temperature. Increasing the value of the time constant with increasing temperature indicates that the adsorption system is endothermic. This parameter cannot be used to determine which equation can best represent the DB-1 and DY-4 adsorption kinetics data on bentonite and bentonite-polysorbate 80, as the time constant values of the PFO and PSO equations are consistent and have the correct physical meaning.

The parameter  $q_e$  is associated with the amount of solute the adsorbent can adsorb under equilibrium conditions. To determine whether the parameter  $q_e$  obtained from the fitting of the data is valid or not, it must be compared with the  $q_e$  obtained from experimental data. From a comparison of the PFO and PSO  $q_e$  parameters with the experimental data, which is also listed in Table 1, it can be seen that the

**Fig. 5** Adsorption kinetics of DB-1 onto **a** bentonite, and **b** bentonite-polysorbate 80

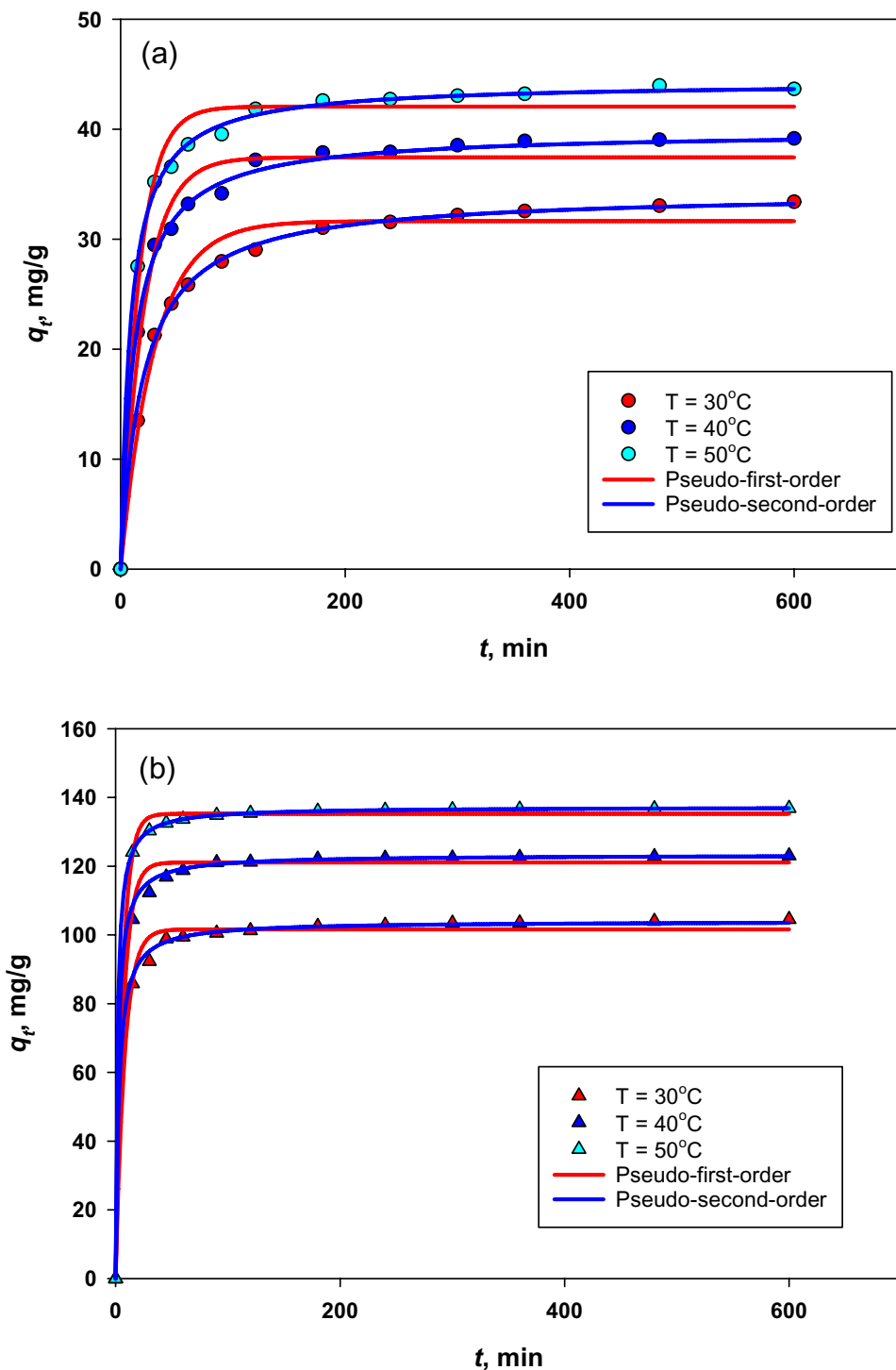


difference between the parameter values of the two equations and the experimental data is small (less than 2%). If the value of  $q_e$  is examined further, the PSO gave a smaller deviation with the experimental data than the PFO for all adsorption systems studied. This evidence indicates that the PSO is more appropriate for representing the kinetics data than the PFO model.

### 3.3 Adsorption Isotherms

The adsorption isotherm (liquid phase) expressed the correlation between concentration at the equilibrium condition and the amount adsorbed by the adsorbent at a specific temperature. The adsorption isotherm is essential information required to design the separation process involving the adsorption process.

**Fig. 6** Adsorption kinetics of DY-4 onto **a** bentonite, and **b** bentonite-polysorbate 80



Many models have been developed to represent the adsorption isotherms for many systems, and two of the most popular are Freundlich and Langmuir equations. Freundlich equation is an empirical equation which has the form as follows:

$$q_e = k_F C_e^{1/n} \tag{6}$$

In the Freundlich equation, the adsorption capacity is usually represented by  $k_F$ , also known as the Freundlich constant. Meanwhile, the system heterogeneity is given by parameter  $n$ , which represents the system heterogeneity.

Langmuir equation was formulated based on several simple assumptions, such as the adsorption occurring in a monolayer, all the adsorption sites are homogeneous in terms of energy, no interaction between adsorbed molecules, and

**Table 1** Parameters of pseudo-first-order and pseudo-second-order equations for adsorption of DB-1 and DY-4 onto (a) bentonite and (b) bentonite-polysorbate 80

Adsorbent	Dye	T, °C	Pseudo-first-order			Pseudo-second-order			$q_e$ exp
			$q_e$ , mg/g	$k_1$ , 1/min	$R^2$	$q_e$ , mg/g	$k_2$ , g/mg.min	$R^2$	
Bentonite	DB-1	30	61.53	0.0717	0.9849	64.41	0.0022	0.9974	64.86
		40	82.13	0.1068	0.9921	84.62	0.0031	0.9989	84.27
		50	106.80	0.1374	0.9961	108.98	0.0039	0.9988	109.71
	DY-4	30	31.65	0.0334	0.9807	34.28	0.0015	0.9978	34.59
		40	37.45	0.0485	0.9807	39.82	0.0021	0.9987	39.05
		50	42.07	0.0617	0.9828	44.29	0.0026	0.9991	43.95
Bentonite-polysorbate 80	DB-1	30	105.83	0.1460	0.9968	107.74	0.0046	0.9989	107.43
		40	125.48	0.1653	0.9981	127.23	0.0052	0.9994	126.83
		50	142.81	0.1830	0.9988	144.36	0.0060	0.9995	143.98
	DY-4	30	101.60	0.1267	0.9949	103.98	0.0035	0.9983	103.81
		40	121.08	0.1461	0.9969	123.27	0.0040	0.9992	124.05
		50	135.23	0.1621	0.9979	137.20	0.0046	0.9994	137.59

the adsorption process is reversible. The Langmuir model is theoretically very suitable if the adsorption isotherm pattern follows type 1 adsorption [14]. Langmuir equation has the following form:

$$q_e = q_{max} \frac{K_L C_e}{1 + K_L C_e} \quad (7)$$

The adsorption capacity of adsorbent toward a specific substance is indicated by parameter  $q_{max}$ , while parameter  $K_L$  represents the adsorption affinity.

Experimental data of DB-1 and DY-4 adsorption isotherms on bentonite and bentonite-polysorbate 80 at various temperatures can be seen in Figs. 7 and 8. Meanwhile, the parameters of Freundlich and Langmuir obtained from fitting the experimental data can be seen in Table 2. Figures 7 and 8 show that the Freundlich equation does not adequately represent the adsorption experimental data at low and high equilibrium concentrations. The deviation between the model and experimental data is relatively small at moderate equilibrium concentrations. This phenomenon is understandable because the weakness of the Freundlich equation is at low and high equilibrium concentrations [14]. The Freundlich equation cannot follow Henry's law at low equilibrium concentrations, whereas the equation does not have a saturation capacity at high concentrations. The Langmuir equation owns both of these, so it can usually represent adsorption equilibrium data for many systems over a wide range of equilibrium concentrations.

In principle, the values of the parameters of the Langmuir equation in Table 2 show consistency. The value of the regression coefficient for the Langmuir equation is also higher than the Freundlich equation, so it can be concluded that the Langmuir equation can represent the experimental data of DB-1 and DY-4 adsorption isotherms on bentonite and bentonite-polysorbate 80.

### 3.4 Binary Adsorption

In industrial wastewater treatment, the adsorption process removes low-concentration contaminants. Usually, these contaminants, especially dyes, rarely occur as a single contaminant. The presence of other contaminants in wastewater will affect the adsorbent's performance due to competition between pollutants, contaminants, solvents, etc. The existence of this competition will cause some of the adsorption sites to remain empty due to the repulsive forces of the contaminant molecules from one another.

Because the Langmuir equation can represent the DB-1 and DY-4 adsorption isotherms on bentonite and bentonite-polysorbate 80, the extended Langmuir equation is used to develop the adsorption isotherm equation for binary adsorption of DB-1 and DY-4. The Langmuir equations for binary adsorption are as follows:

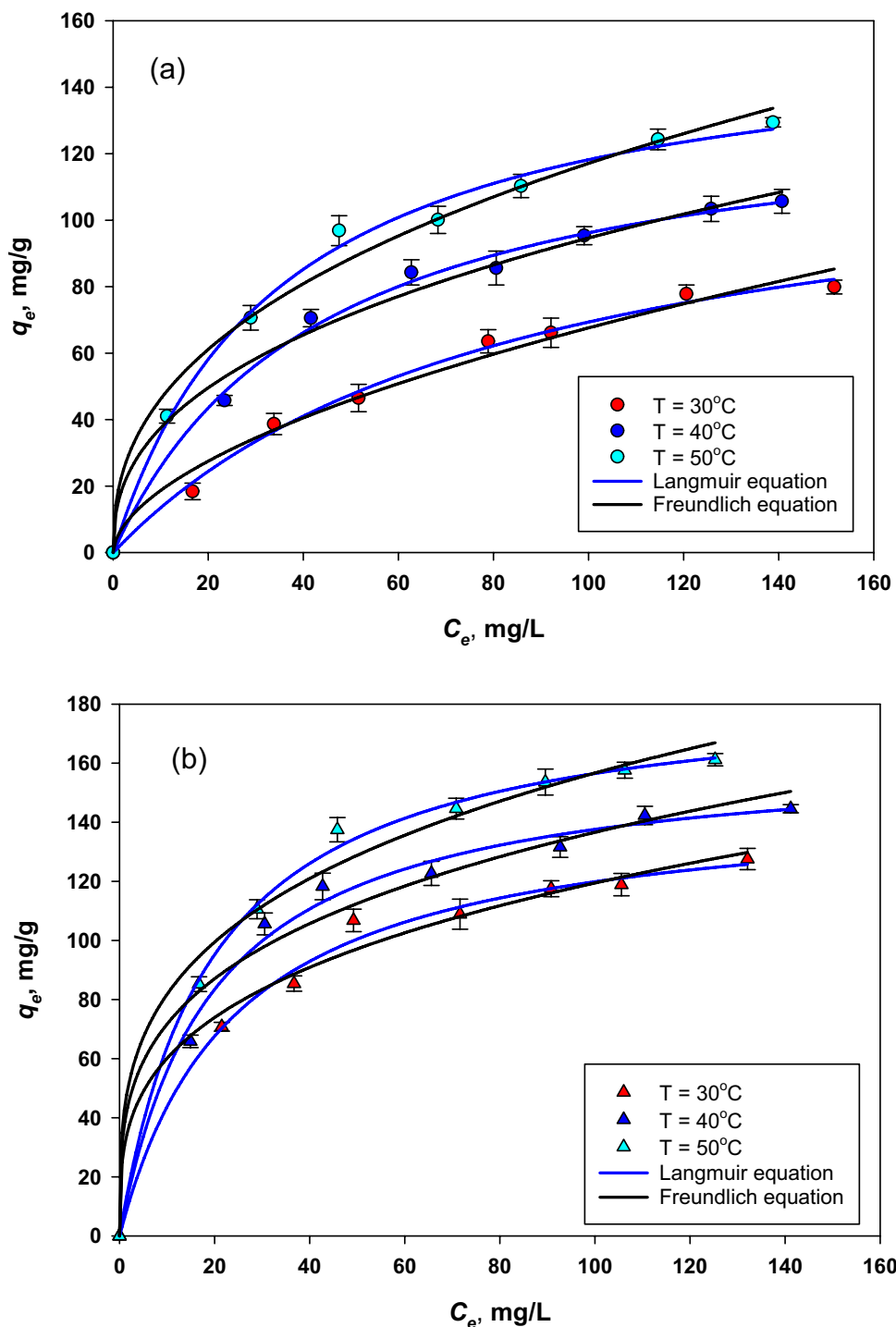
$$q_{e,1} = \frac{q_{max,1} K_{L,1} C_{e,1}}{1 + K_{L,1} C_{e,1} + K_{L,2} C_{e,2}} \quad (8)$$

$$q_{e,2} = \frac{q_{max,2} K_{L,2} C_{e,2}}{1 + K_{L,1} C_{e,1} + K_{L,2} C_{e,2}} \quad (9)$$

$q_m$  and  $K_L$  are Langmuir parameters for single components; the values of these parameters can be seen in Table 2.

Implementing the extended Langmuir equation to represent experimental data for binary adsorption DB-1 and DY-4 requires the Langmuir equation parameters obtained from single component adsorption. Using the extended Langmuir equation directly to represent binary adsorption data is often less accurate, so it is necessary to modify the equation. In this study, all Langmuir parameters for a single component have a high correlation coefficient; however, when applied with the extended Langmuir equation,

**Fig. 7** Adsorption isotherm of DB-1 onto **a** bentonite and **b** bentonite-polysorbate 80

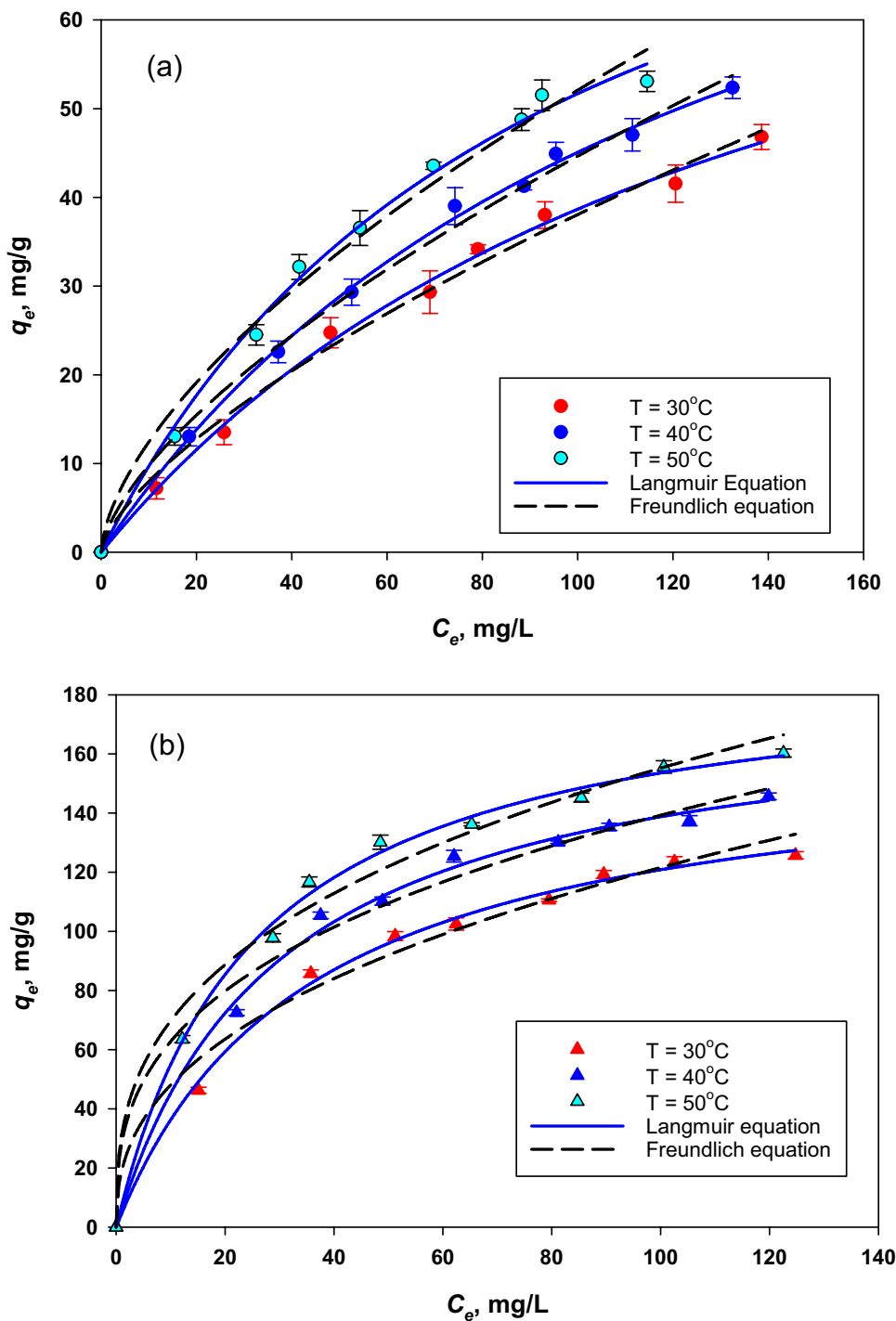


they cannot represent binary adsorption data DB-1 and DY-4 well (Fig. 9).

Figure 9 reveals that the results of calculating the adsorption isotherms of the binary compounds DB-1 and DY-4 using the extended Langmuir equation are significantly higher than the experimental results. The extended Langmuir equation does not consider competition between

adsorbed molecules. This competition between molecules will impact the system's adsorption affinity. The existence of this competition will cause the number of adsorbed adsorbate molecules to be lower. This phenomenon is not included in the extended Langmuir equation. Because the competition typically affects adsorption affinity, the adsorption affinity parameter is modified as follows:

**Fig. 8** Adsorption isotherm of DY-4 onto **a** bentonite and **b** bentonite-polysorbate 80



$$K_{L,1bin} = K_{L,1}(1 - \exp(-A_{12})) \tag{10}$$

And

$$K_{L,2bin} = K_{L,2}(1 - \exp(-A_{21})) \tag{11}$$

where  $A_{12}$  and  $A_{21}$  are competition coefficients. The final forms of the modification extended Langmuir model are given in Eqs. (12) and (13).

$$q_{e,1} = \frac{q_{max,1}K_{L,1}(1 - \exp(-A_{12}))C_{e,1}}{1 + K_{L,1}(1 - \exp(-A_{12}))C_{e,1} + K_{L,2}(1 - \exp(-A_{21}))C_{e,2}} \tag{12}$$

$$q_{e,2} = \frac{q_{max,2}K_{L,2}(1 - \exp(-A_{21}))C_{e,2}}{1 + K_{L,1}(1 - \exp(-A_{12}))C_{e,1} + K_{L,2}(1 - \exp(-A_{21}))C_{e,2}} \tag{13}$$

**Table 2** Parameters of Langmuir and Freundlich equations for adsorption of DB-1 and DY-4 onto (a) bentonite and (b) bentonite-polysorbate 80

Adsorbent	Dye	T, °C	Langmuir			Freundlich		
			$q_{max}$ , mg/L	$K_L$ , L/mg	$R^2$	$K_F$ , (mg/g) (L/mg) <sup>1/n</sup>	$n$	$R^2$
Bentonite	DB-1	30	128.26	0.0118	0.995	5.17	1.79	0.9820
		40	137.4	0.0231	0.995	14.89	2.49	0.987
		50	159.31	0.0288	0.994	18.25	2.48	0.987
	DY-4	30	93.22	0.0051	0.997	1.68	1.47	0.992
		40	99.42	0.0077	0.998	2.15	1.52	0.994
		50	103.55	0.084	0.995	2.97	1.61	0.986
Bentonite-polysorbate 80	DB-1	30	148.56	0.0418	0.993	30.28	3.35	0.987
		40	164.23	0.0517	0.992	37.65	3.57	0.975
		50	186.55	0.0581	0.998	42.70	3.54	0.987
	DY-4	30	163.12	0.0206	0.997	19.02	2.48	0.983
		40	180.10	0.0336	0.996	28.33	2.89	0.987
		50	191.83	0.0401	0.996	31.33	2.87	0.984

The values of  $A_{12}$  and  $A_{21}$  for each adsorbent were obtained by interpreting binary adsorption data using Eqs. (12) and (13) by the non-linear least square method. All the binary isotherm data in one adsorbent were jointly fitted using Eqs. (12) and (13) simultaneously. The residual sum of squares (RSS) was employed as the objective equation to be minimized to achieve the target.

$$RSS = \sum_{i=1}^n \sum_{j=1}^m (Q_{ij} - q_{ij})^2 \quad (14)$$

The symbols  $q_{ij}$  and  $Q_{ij}$  in Eq. (12) represent the experimental amount of dyes adsorbed and the predicted amount of dyes adsorbed, respectively.

Because the extended Langmuir equation failed to describe binary adsorption data DB-1 and DY-4 on bentonite adequately, this equation was not used further to correlate binary adsorption data DB-1 and DY-4 on bentonite-polysorbate 80 composites. To demonstrate the ability of the modified Langmuir extended equation to represent binary adsorption data, this equation was used to describe experimental data of DB-1 and DY-4 binary adsorption on bentonite and bentonite-polysorbate 80. Binary adsorption data for the two dyes on bentonite and their modifications were obtained at 30 °C with an initial concentration of 100 mg/L for each dye. The results of theoretical calculations using the modified Langmuir extended equation and experimental data can be seen in Figs. 10 and 11.

The values for parameters  $A_{12}$  and  $A_{21}$  obtained for the DB-1 and DY-4 systems on bentonite are 0.3510 and 0.8902, with a correlation coefficient ( $R^2$ ) of 0.9142. Meanwhile, for the DB-1 and DY-4 systems on bentonite-polysorbate 80, parameters  $A_{12}$  and  $A_{21}$  were 0.4776 and 0.8841, respectively, with a correlation coefficient ( $R^2$ ) of 0.9344 (Table 3). The values of parameter  $A_{12}$  for both adsorbents are smaller

than  $A_{21}$ . Based on Eqs. (10) and (11), a small value of the competition coefficient will give a higher value of adsorption affinity  $K_L$ . From the values of  $A_{12}$  and  $A_{21}$  for both adsorbents, it can be concluded that DB-1 is more competitive than DY-4 toward the surface of both adsorbents. Visually, the modification of  $K_L$  values significantly impacts the validity of the extended Langmuir equation in correlating binary adsorption experimental data.

As previously explained, in binary system adsorption, competition occurs between adsorbates to fight over available adsorption sites on the surface of the adsorbent. The attractive forces occur between the adsorbate and the adsorbent, as well as the repulsive forces between the adsorbate molecules. This phenomenon will weaken the interaction between the adsorbate and the adsorbent; the value of the  $K_L$  parameter will decrease with the competition between the adsorbate molecules. This phenomenon cannot be captured by the original Langmuir extended. Modifying the  $K_L$  value by adding a competition factor allows the Langmuir extended equation to represent the DB-1 and DY-4 binary adsorption data on bentonite and bentonite-polysorbate 80 well.

From the experimental results of DB-1 and DY-1 adsorption on bentonite and bentonite-polysorbate 80 composites for both single-component and binary-component sorption, it can be seen that DB-1 is more easily adsorbed on both adsorbents. DB-1 has a larger molecular weight than DY-4, and with a larger molecular weight, the molecular size of DB-1 is also larger than that of DY-4. In the adsorption process, there is a force, namely the attractive force, that can attract adsorbate molecules to be bound to the adsorbent surface. Several factors influence this attractive force; among them is the size of the adsorbate molecule. The larger the molecular size, the greater the attractive force experienced by the adsorbate molecule to attach to the adsorbent surface.

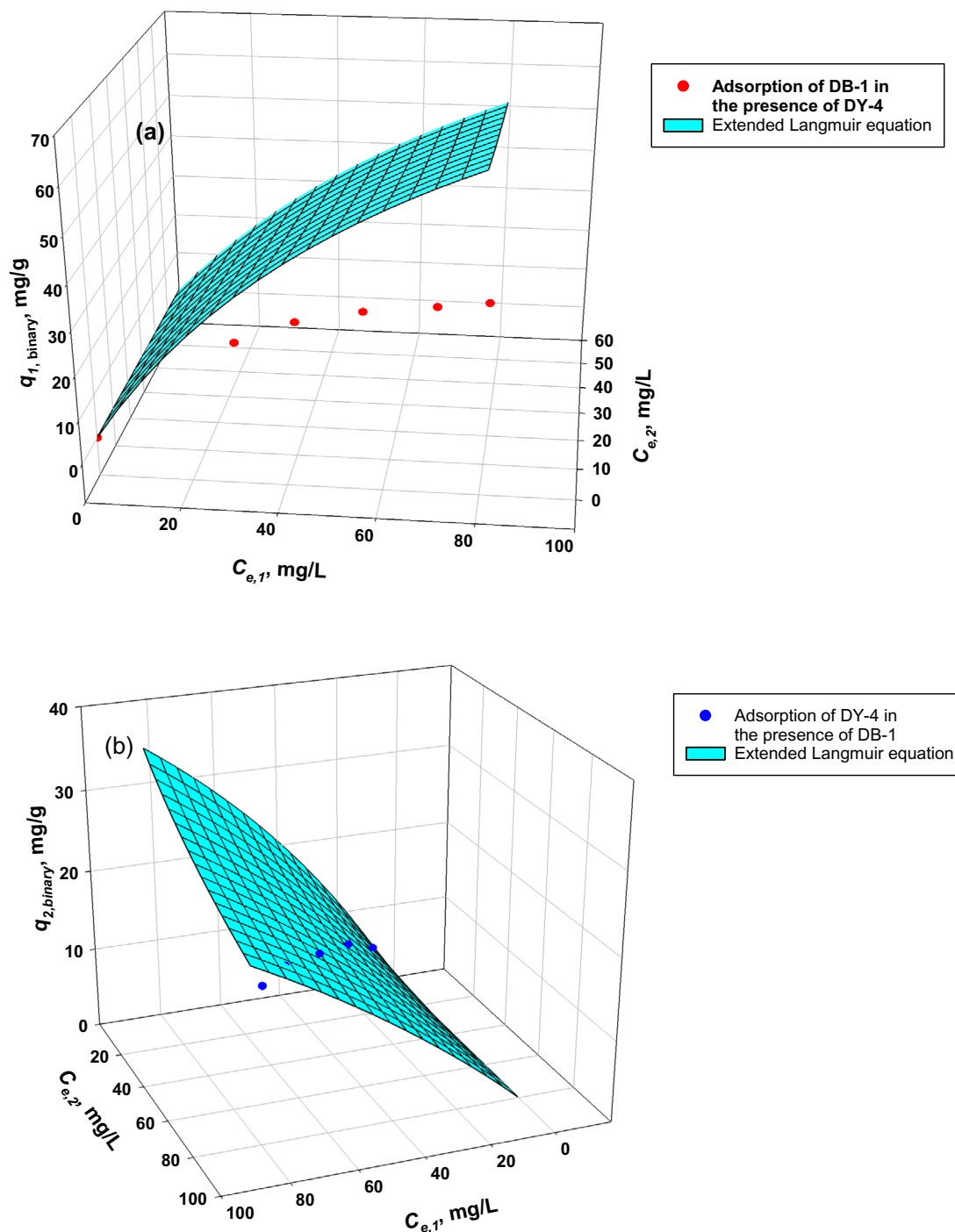


**Fig. 9** Binary adsorption of binary compounds of DB-1 and DY-4 on bentonite, mesh curve is original extended Langmuir model (initial concentration of DB-1 and DY-4 is 100 mg/L,  $T=30\text{ }^{\circ}\text{C}$ )

Since the molecular size of DB-1 is larger than DY-4, due to the influence of this attractive force, DB-1 is automatically more and readily adsorbed on the surface of bentonite and bentonite-polysorbate 80 composite.

The results obtained in this study show that the competition factor is quite crucial for the adsorption process

in binary systems. The amount of each dye (DB-1 and DY-4) adsorbed on bentonite and bentonite-polysorbate 80 decreased compared to the single compound adsorption process. The results align with several dye adsorption studies on various adsorbents [3, 23, 28]. Sellaoui et al. [23] studied the adsorption of DB-1 and DY-4 onto HKUST-1,

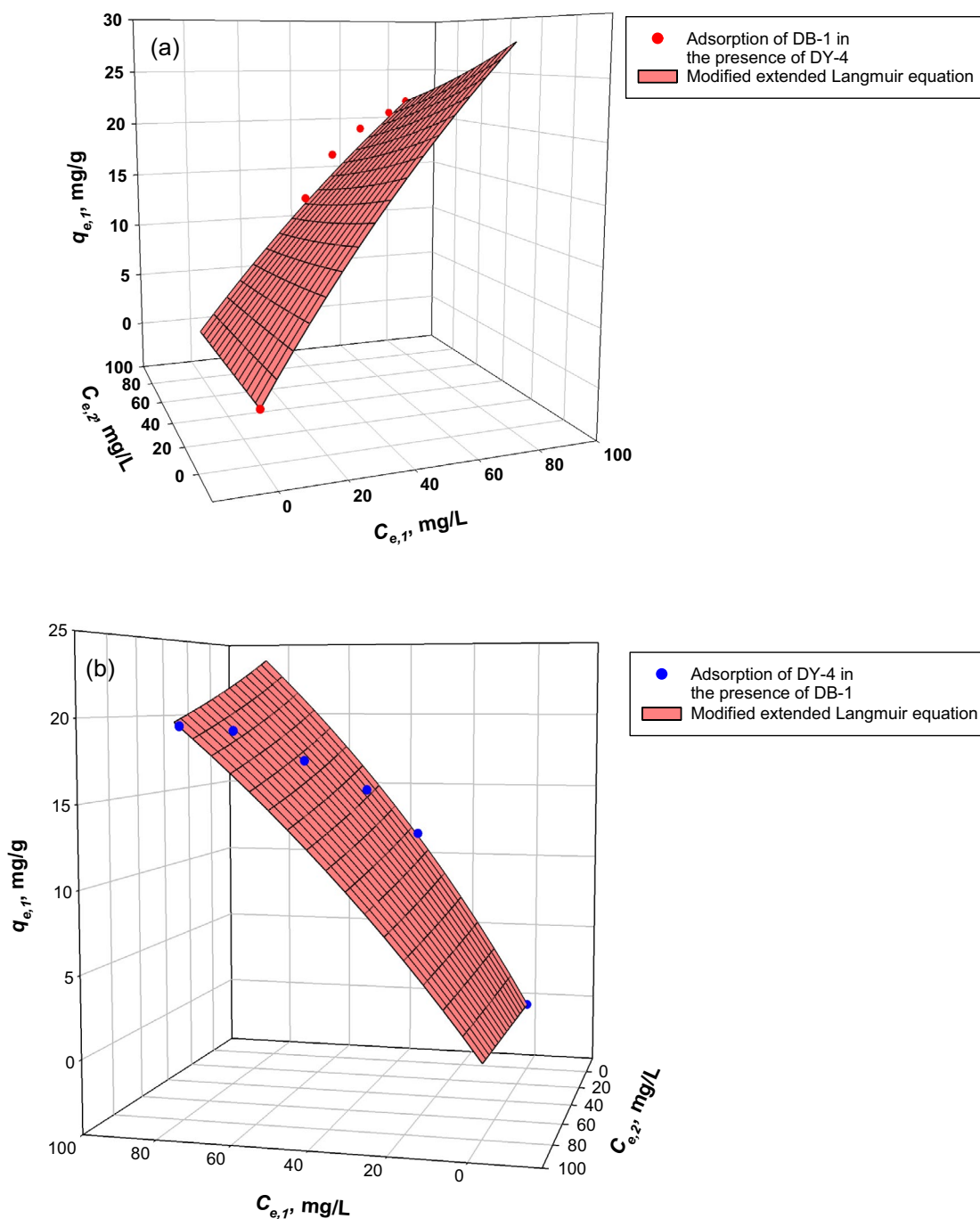


**Fig. 10** Binary adsorption of binary compounds of DB-1 and DY-4 on bentonite, mesh curve is modified extended Langmuir model (initial concentration of DB-1 and DY-4 is 100 mg/L,  $T=30\text{ }^{\circ}\text{C}$ )

and they also found that the adsorption of DB-1 was higher than that of DY-4. Based on the statistical physic analysis, they observed that the dye molecules were removed from the water solution without undergoing molecular aggregation. DB-1 was absorbed through a non-parallel orientation, whereas DY-4 dye was absorbed through a combination of orientations [23].

## 4 Conclusions

Intercalation of bentonite using polysorbate 80 has changed the basal spacing of bentonite from 1.54 to 1.66 nm. Increasing the basal spacing also increases the adsorption capacity of organo-bentonite (bentonite-polysorbate 80) on two basic dyes, DB-1 and DY-4. The adsorption kinetics of DB-1 and

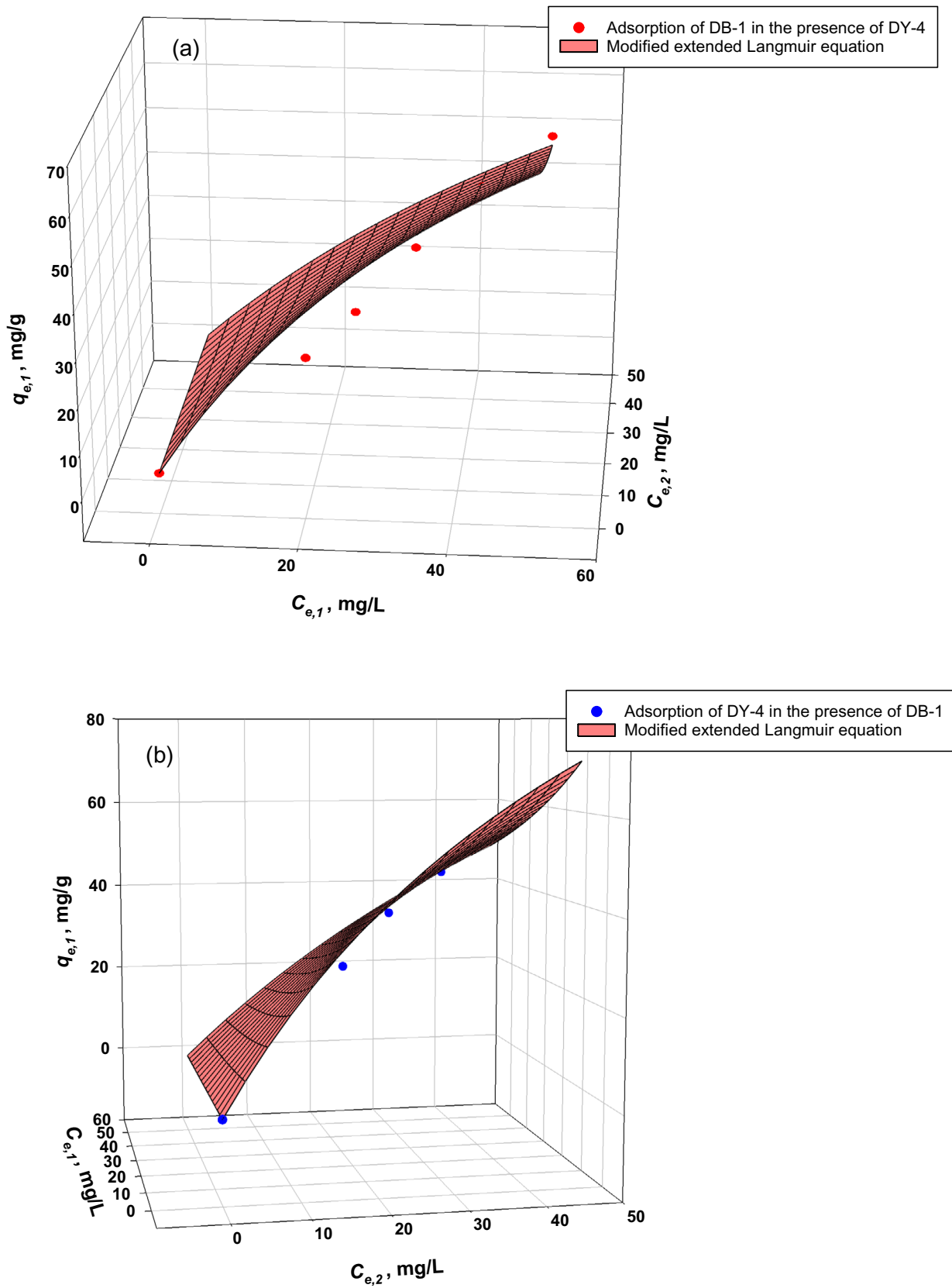


**Fig. 11** Binary adsorption of binary compounds of DB-1 and DY-4 on bentonite-polysorbate 80, mesh curve is modified extended Langmuir model (initial concentration of DB-1 and DY-4 is 100 mg/L,  $T=30\text{ }^{\circ}\text{C}$ )

**Table 3** Parameters of modified extended Langmuir model for adsorption of DB-1 and DY-4 at 30 °C

Adsorbent	$A_{12}$	$A_{21}$	$R^2$	$K_{L,1 \text{ bin}}$	$K_{L,2 \text{ bin}}$
Bentonite	0.3510	0.8902	0.9142	0.0035	0.0029
Bentonite-polysorbate 80	0.4776	0.8841	0.9344	0.0159	0.0121

DY-4 on bentonite and its composites are described using the PFO and PSO equations. The PSO equation better represents the adsorption kinetics of the studied systems than the PFO equations. The Langmuir equation can represent the DB-1 and DY-4 adsorption isotherms on bentonite and bentonite-polysorbate 80. In binary system adsorption, the adsorbates compete with each other for available adsorption sites on the surface of the adsorbent. In addition to the attractive forces between the adsorbate and the adsorbent, there are repulsive forces between the adsorbate molecules. Adding a correction factor in the form of competition to the  $K_L$  value can accurately modify Langmuir's extended equation to represent binary adsorption data DB-1 and DY-4 on bentonite and bentonite-polysorbate 80.

**Acknowledgements** This study was supported by the Institute for Research and Community Service, Widya Mandala Surabaya Catholic University, through the Internal Research Scheme 2022.

**Author Contributions** Conceptualization: Suryadi Ismadji, Jindrayani Nyoo Putro; Data curation: Jindrayani Nyoo Putro, Christian Julius Wijaya, Shella Permatasari Santoso; Formal analysis: Chintya Gunarto, Jaka Sunarso, Agus Saptor, Sanggono Adisasmito; Funding acquisition: Jindrayani Nyoo Putro, Felycia Edi Soetaredjo; Investigation: Jindrayani Nyoo Putro, Christian Julius Wijaya, Shella Permatasari Santoso; Methodology; Project administration; Resources: Suryadi Ismadji, Felycia Edi Soetaredjo, I Gede Wenten; Validation: Jaka Sunarso, Agus Saptor; Roles/Writing—original draft: Jindrayani Nyoo Putro; and Writing—review and editing: Suryadi Ismadji, I Gede Wenten.

**Data availability** The data will be available upon request.

## Declarations

**Conflict of Interest** The authors declare that they have no known competing financial and conflict of interests or personal relationships that could have appeared to influence the work reported in this paper.

## References

- Ahmad R (2023) Ejaz, MO Efficient adsorption of crystal violet (CV) dye onto benign chitosan-modified L-cysteine/bentonite (CS-Cys/Bent) bionanocomposite: synthesis, characterization and experimental studies. *Dyes Pigment* 216:111305. <https://doi.org/10.1016/j.dyepig.2023.111305>
- Ali B, Naceur B, Tewfik A-D, Nourredine B (2024) Simultaneously removal of indigo carmine and Congo Red anionic dyes from aqueous solutions using nickel-chromium and zinc-chromium layered double hydroxides. *Anal Bioanal Chem Res* 11:309–326. <https://doi.org/10.22036/abc.2024.440346.2040>
- Achour Y, Khouili M, Abderrafia H, Melliani S, Laamari MR, El Haddad M (2018) DFT investigations and experimental studies for competitive and adsorptive removal of two cationic dyes onto an eco-friendly material from aqueous media. *Int J Environ Res* 12:789–802. <https://doi.org/10.1007/s41742-018-0131-x>
- Belcaid A, Beakou BH, Bouhsina S, Anouar A (2023) New insights on manganese dioxide nanoparticles loaded on cellulose-based biochar of cassava peel for the adsorption of three cationic dyes from wastewater. *Int J Biol Macromol* 241:124534. <https://doi.org/10.1016/j.ijbiomac.2023.124534>
- Benamer-Oudih S, Tahtat D, Nacer Khodja A, Mansouri B, Mahlous M, Guittoum AE, Kebbouche Gana S (2024) Sorption behavior of chitosan nanoparticles for single and binary removal of cationic and anionic dyes from aqueous solution. *Environ Sci Pollut Res* 31:39976–39993
- Bide Y, Fashapoyeh MA, Shokrollahzadeh S (2021) Structural investigation and application of Tween 80-choline chloride self-assemblies as osmotic agent for water desalination. *Sci Rep* 11:17068. <https://doi.org/10.1038/s41598-021-96199-6>
- Blanchard G, Maunaye M, Martin G (1984) Removal of heavy metals from waters by means of natural zeolites. *Water Res* 18:1501–1507. [https://doi.org/10.1016/0043-1354\(84\)90124-6](https://doi.org/10.1016/0043-1354(84)90124-6)
- Cuevas J, Cabrera MA, Fernández C, Mota-Herencia C, Fernández R, Torres E, Turrero MJ, Ruiz AI (2022) Bentonite powder XRD quantitative analysis using Rietveld refinement: revisiting and updating bulk semiquantitative mineralogical compositions. *Minerals* 12:772. <https://doi.org/10.3390/min12060772>
- Cui GY, Zhang W, Yang JM (2023) Selective adsorptive removal of anionic dyes from aqueous solutions using MIL-101@GO: effect of GO. *Colloids Surf A Physicochem Eng Asp* 667:131364. <https://doi.org/10.1016/j.colsurfa.2023.131364>
- El-Sheikh AH, Saadeh EA, Abdelghani JI (2023) The use of various magnetic adsorbents for cadmium uptake from dyes-containing wastewater. *Emerg Contam* 9:100227. <https://doi.org/10.1016/j.emcon.2023.100227>
- Heidari Y, Noroozian E, Maghsoudi S (2023) Electrospun nanofibers of cellulose acetate/metal organic framework-third generation PAMAM dendrimer for the removal of methylene blue from aqueous media. *Sci Rep* 13:4924. <https://doi.org/10.1038/s41598-023-32097-3>
- Hua Y, Xu D, Liu Z, Zhou J, Lin JZ, Xu D, Chen G, Huang X, Chen J, Lv J, Liu G (2023) Effective adsorption and removal of malachite green and Pb<sup>2+</sup> from aqueous samples and fruit juices by pollen-inspired magnetic hydroxyapatite nanoparticles/hydrogel beads. *J Clean Prod* 411:137233. <https://doi.org/10.1016/j.jclepro.2023.137233>
- Ismadji S, Soetaredjo FE, Ayucitra A (2015) Clay materials for environmental remediation. Springer International Publishing AG, Cham. <https://doi.org/10.1007/978-3-319-16712-1>
- Kurniawan A, Sutiono H, Ju YH, Soetaredjo FE, Ayucitra A, Yudha A, Ismadji S (2011) Utilization of rarasaponin natural surfactant for organo-bentonite preparation: application for methylene blue removal from aqueous effluent. *Microporous Mesoporous Mater* 142:184–193. <https://doi.org/10.1016/j.micromeso.2010.11.032>
- Lagergren S (1898) Zur theorie der sogenannten adsorption gelöster stoffe Kungliga Svenska Vetenskapsakademiens. *Handlingar* 24:1–39
- Ma Y, Jiang X, Liu Z, Geng L, Zhang X, Niu P, Zhang X, Zhang Y, Zhang D, Hu H, Li X, Wang X (2023) Combining hierarchical pores and unsaturated sites into Quasi-MIL-125(Ti) for ultra-fast and efficient adsorption of cationic dyes. *Polyhedron* 239:116430. <https://doi.org/10.1016/j.poly.2023.116430>

17. Mahmoud ME, Abdelwahab MS, Ibrahim GAA (2023) Surface functionalization of magnetic graphene oxide@bentonite with  $\alpha$ -amylase enzyme as a novel bionanosorbent for effective removal of Rhodamine B and Auramine O dyes. *Mater Chem Phys* 301:127638. <https://doi.org/10.1016/j.matchemphys.2023.127638>
18. Moustafa MT (2023) Preparation and characterization of low-cost adsorbents for the efficient removal of malachite green using response surface modeling and reusability studies. *Sci Rep* 13:4493. <https://doi.org/10.1038/s41598-023-31391-4>
19. Oviedo LR, Oviedo VR, Dalla Nora LD, da Silva WL (2023) Adsorption of organic dyes onto nanozeolites: a machine learning study. *Sep Purif Technol* 315:123712. <https://doi.org/10.1016/j.seppur.2023.123712>
20. Pang X, Sellaoui L, Franco D, Dotto GL, Georgin J, Bajahzar A, Belmabrouk H, Lamine AB, Bonilla-Petriciolet A, Li Z (2019) Adsorption of crystal violet on biomasses from pecan nutshell, para chestnut husk, araucaria bark and palm cactus: experimental study and theoretical modeling via monolayer and double layer statistical physics models. *Chem Eng J* 378:122101. <https://doi.org/10.1016/j.cej.2019.122101>
21. Sajid M, Ihsanullah I (2023) Magnetic layered double hydroxide-based composites as sustainable adsorbent materials for water treatment applications: progress, challenges, and outlook. *Sci Total Environ* 880:163299. <https://doi.org/10.1016/j.scitotenv.2023.163299>
22. Salama E, Ossman M, Hamdy A, Shokry H, Elkady MF (2023) Magnetic MOF composite material for decontamination of direct red 81 from polluted water. *AIP Adv* 13:025349. <https://doi.org/10.1063/9.0000529>
23. Sellaoui L, Edi-Soetaredjo F, Mohamed M, Ismajji S, Ernst B, Bonilla-Petriciolet A, Ben Lamine A, Dell'Angelo D, Badawi M (2024) A novel application of HKUST-1 for textile dyes removal in single and binary solutions: experimental investigation combined with physical modelling. *Chem Eng J* 480:147958. <https://doi.org/10.1016/j.cej.2023.147958>
24. Taibi Z, Bentaleb K, Bouberka Z, Pierlot C, Vandewalle M, Volkringer C, Supiot P, Maschke U (2023) Adsorption of Orange G dye on hydrophobic activated bentonite from aqueous solution. *Crystals* 13:211. <https://doi.org/10.3390/cryst13020211>
25. Wang X, Xu Q, Zhang L, Pei L, Xue H, Li Z (2023) Adsorption of methylene blue and Congo red from aqueous solution on 3D MXene/carbon foam hybrid aerogels: A study by experimental and statistical physics modeling. *J Environ Chem Eng* 11:109206. <https://doi.org/10.1016/j.jece.2022.109206>
26. Yang X, Shao X, Tong J, Zhou J, Feng Y, Chen R, Yang Q, Han Y, Yang X, Wang L, Ma X, Fan Z, Song Z, Zimmerman AR, Gao B (2023) Removal of aqueous eriochrome blue-black R by novel Na-bentonite/hickory biochar composites. *Sep Purif Technol* 311:123209. <https://doi.org/10.1016/j.seppur.2023.123209>
27. Yadav S, Chander S, Luhach N, Kashyap A, Gupta A (2024) Binary color adsorption by zinc@magnetite nanocomposites: robust parametric optimization using Taguchi method. *Vietnam J Chem* 62:328–336. <https://doi.org/10.1002/vjch.202300318>
28. Yazid H, Bouzid T, Regti A, El Himri M, El Haddad M (2024) Experimental and DFT insights into the adsorption competition of two cationic dyes on activated carbon derived from walnut shells in aqueous solutions. *Environ Nanotechnol Monit Manag* 21:100940. <https://doi.org/10.1016/j.enmm.2024.100940>
29. Zeinali N, Ghaedi M, Shafie G (2014) Competitive adsorption of methylene blue and brilliant green onto graphite oxide nano particle following: derivative spectrophotometric and principal component-artificial neural network model methods for their simultaneous determination. *J Ind Eng Chem* 20:3550–3558. <https://doi.org/10.1016/j.jiec.2013.12.048>
30. Zhang LL, Zaoui A, Sekkal W, Zheng YY (2023) Interlayer adsorption of cationic dye on cationic surfactant-modified and unmodified montmorillonite. *J Hazard Mater* 442:130107. <https://doi.org/10.1016/j.jhazmat.2022.130107>
31. Zheng L, Sun L, Qiu J, Song J, Zou L, Teng Y, Zong Y, Yu H (2024) Using NH<sub>2</sub>-MIL-125(Ti) for efficient removal of Cr(VI) and RhB from aqueous solutions: Competitive and cooperative behavior in the binary system. *J Environ Sci* 136:437–450. <https://doi.org/10.1016/j.jes.2023.02.013>
32. Zhu Y, Cui Y, Peng Y, Dai R, Chen H, Wang Y (2023) Preparation of CTAB intercalated bentonite for ultrafast adsorption of anionic dyes and mechanism study. *Colloids Surf A Physicochem Eng Asp* 658:130705. <https://doi.org/10.1016/j.colsurfa.2022.130705>

Springer Nature or its licensor (e.g. a society or other partner) holds exclusive rights to this article under a publishing agreement with the author(s) or other rightsholder(s); author self-archiving of the accepted manuscript version of this article is solely governed by the terms of such publishing agreement and applicable law.